Ferroelectric Problem beyond the Conventional Scaling Law

Qi-Jun Ye,[1] Zhi-Yuan Liu,[1] Yexin Feng,[2] Peng Gao,[3,4] and Xin-Zheng Li[1,4,*]
[1]State Key Laboratory for Artificial Microstructure and Mesoscopic Physics, and School of Physics, Peking University, Beijing 100871, People's Republic of China
[2]School of Physics and Electronics, Hunan University, Changsha 410082, People's Republic of China
[3]International Center for Quantum Materials, and Electron Microscopy Laboratory, School of Physics, Peking University, Beijing 100871, People's Republic of China
[4]Collaborative Innovation Center of Quantum Matter, Peking University, Beijing 100871, People's Republic of China

(Received 17 May 2018; published 26 September 2018)

Ferroelectric (FE) size effects against the scaling law were reported recently in ultrathin group-IV monochalcogenides, and extrinsic effects (e.g., defects and lattice strains) were often resorted to. Via first-principles based finite-temperature (T) simulations, we reveal that these abnormalities are intrinsic to their unusual symmetry breaking from bulk to thin film. Changes of the electronic structures result in different order parameters characterizing the FE phase transition in bulk and in thin films, and invalidation of the scaling law. Beyond the scaling law T_c limit, this mechanism can help predict materials that are promising for room-T ultrathin FE devices of broad interest.

DOI: 10.1103/PhysRevLett.121.135702

Miniaturized ferroelectric (FE) devices in continued demand for portable consumer electron electronics require a prerequisite understanding of a fundamental question, i.e., the nature of FE size effects [1–6]. Finite size scaling (FSS) theory, as the conventional wisdom, predicts that the Curie temperature T_c for the paraelectric (PE) to FE phase transitions decreases when scaling down to finite sizes [7–9] as follows:

$$\delta T_c(d) = \frac{T_c(\infty) - T_c(d)}{T_c(\infty)} = \left(\frac{\xi_0}{d}\right)^{\lambda}, \qquad (1)$$

where ξ_0 is the character length, λ is the universal critical exponent, and $T_c(d)$ and $T_c(\infty)$ are the T_c of the film of thickness d and bulk, respectively [10]. The key point is the truncated long-range correlations by finite size, upon which the low-dimensional system requires lower T_c to stabilize its polarization [7,11]. As FSS theory has been predictive in perovskites and a variety of FEs [1,12–14], $T_c(d)$ being lower in ultrathin films was believed heretofore as an essential limit in realizing room temperature (T) ultrathin FE devices of broad interest [2,12].

Recent studies on group-IV monochalcogenides, however, opened the door for realization of room-T ultrathin FE devices beyond the FSS theory prediction [15–20]. The experiment by K. Chang *et al.* showed that in one unit-cell (1UC) SnTe film the Curie temperature ($T_c^{1\mathrm{UC}}$) is 270 K [15], enhanced from the bulk value (T_c^{bulk}) of 98 K [21]. Parallel to this, Fei *et al.* predicted robust ferroelectricity in analogous monolayer group-IV monochalcogenides MX (M = Ge, Sn; X = S, Se) via the Landau-Ginzburg-type effective Hamiltonian method [16]. Wu and Zeng showed MX's multiferroelectricity, where the polarization valley switching by using stress or electric field enables designing room-T nonvolatile memory [17,22]. Nevertheless, large extrinsic effects claimed in these studies such as lower free carrier density [15,18,23,24], lattice strains [19,25,26], etc., render the intrinsic size effect of ferroelectricity unimportant, thereby hindering further investigation and searching for other promising materials.

In this Letter, we address two issues: (i) reveal the nature of intrinsic FE size effects in these materials and analyze their relations with the FSS theory, and (ii) propose an easy-to-use criteria for potential low-dimensional FE materials with T_c higher than their high-dimensional correspondences. SnTe and $BaTiO_3$ (BTO), two paradigmatic FE materials whose scaling behaviors show remarkable difference, are discussed in detail. Based on the first-principles exploration of potential energy surfaces, an effective Hamiltonian is built and used in Monte Carlo simulations, to investigate the finite-T PE-FE phase transitions. Our simulations reproduce the experimental results of robust in-plane ferroelectricity and abnormal thickness dependency of the T_c in SnTe films, and the conventional scaling behaviors in BTO films. The key factor to understand this fundamental difference is that in SnTe the order parameters are deviated for the three-dimensional (3D) and two-dimensional (2D) PE-FE phase transitions, while in BTO no deviation occurs. As this can be perceived macroscopically by jumping phases in the PE-FE transition, a rule of thumb is proposed to predict analogous low-dimensional FE materials.

We adopt the model proposed by Vanderbilt and coworkers [27,28], which enables large-scale calculations

with first-principles predictive power, to investigate the FE phase transitions in bulk and thin films of SnTe and BTO. This method is formerly and successfully applied to bulk perovskites including BTO [29–34]. Because of the same displacive feature, i.e., soft optical modes (so-called FE modes) driving spontaneous polarization below T_c, this method can be freely extended to group-IV monochalcogenides including SnTe. The total energy of an instantaneous finite-T structure differing from the chosen high-symmetry reference structure is written as

$$E_{\mathrm{tot}}^{(d_m)} = E_{\mathrm{ref}} + E_{\mathrm{3D\text{-}param}}^{(d_m)}(\{\mathbf{u}_i\}, \eta, p) + E_{\mathrm{corr}}^{(d_m)}, \quad (2)$$

where d_m labels the dimension of the system, $\mathbf{u}_i$ describes the FE modes at ith site, η is the homogeneous strain tensor, and p is the hydrostatic pressure coupled with the diagonal terms of η. $E_{\mathrm{3D\text{-}param}}^{d_m}$ contains the intra- and interactions of the dominant soft modes (FE modes here) and the lattice strains, parametrized in 3D structure. The specific form of the first two terms can be found in Refs. [27] and [35], and a schematic of one finite-T instantaneous FE mode configuration on the strained lattice is shown in Fig. S1. In order to describe the FE properties in film geometry, we make improvements based on the original Hamiltonian in Ref. [27]: (i) EW2D method is used to correctly treat the long-range interactions of dipoles in the truncated geometry of films [44]; (ii) the correction term $E_{\mathrm{corr}}^{(d_m)}$ is added only for the 2D and one-dimensional (1D) systems to address the changes of the electronic structures upon decreasing dimensionality, as we show later in Fig. 2. For ultrathin films (2D systems), we adopt a correction of exponential decay on the film thickness, analogous to the form of Ref. [45], as

$$E_{\mathrm{corr}}^{(\mathrm{2D})}(n_l) = \sum_{\substack{\alpha=\beta \\ \alpha=x,y}} \sum_{\substack{\langle i,j\rangle \\ j=i\pm\hat{\alpha}}} e^{-Bn_l} A_{ij,\alpha\beta} u_{i\alpha} u_{j\beta}, \quad (3)$$

where n_l labels the number of layers, and $A_{ij,\alpha\beta}$ describes the short-range interactions (exclude the short part of dipole-dipole interactions) between neighboring sites $\langle i, j\rangle$. Parameters for Eqs. (2) and (3) are derived from first-principles explorations of the potential energy profiles of the 3D and 2D systems, respectively. For more computation details please see Supplemental Material [35].

FE modes, the key instabilities for a system going from high-symmetry PE phase to symmetry-breaking FE phase, can be viewed as the order parameters in this process. In fact, it is a good approximation shown by Refs. [46] and [47] that the polarization at one unit site ($\mathbf{P}_i$) is almost linear to the FE mode magnitude, through

$$\mathbf{P}_i = eZ_{\mathrm{Born}}^{*}\mathbf{u}_i/V. \quad (4)$$

Z_{Born}^{*} is the Born charge and V is the cell volume. We use $u_{x,y,z} = \langle u_i \rangle_{x,y,z}$ to characterize the phase transition. The

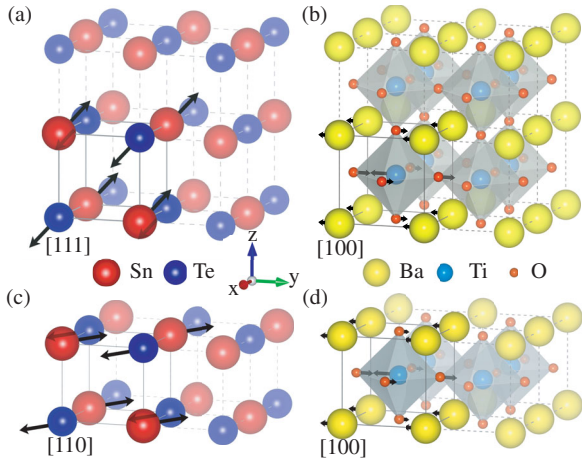

FIG. 1. The responsible FE modes associated with the FE phase in (a) bulk SnTe, (b) bulk BTO, (c) 1UC SnTe film, and (d) 1UC BTO film (Ba-O terminated). The black arrows sketch the atomic displacement patterns of the FE modes.

responsible FE modes for the 3D and 2D structures are different in SnTe, and they are the same in BTO. Polarization along [111] in 3D SnTe [Fig. 1(a)], namely, the rhombohedral FE phase, is a result of simultaneous softening of the triply degenerate FE modes u_x, u_y, and u_z. While in 2D SnTe [Fig. 1(c)], it is the polarization along [110] and the softening of the doubly degenerate in-plane FE modes u_x and u_y that characterize the PE-FE transition. In BTO [Figs. 1(b) and 1(d)], the polarization along [100] and a singlet FE mode is the order parameter, and it does not change in the 3D and 2D systems [48]. This unusual symmetry breaking in SnTe might be a clue to its abnormal scaling behavior.

We start discussions by looking at the static energies. Taking the cubic structure as reference, we arrange the Sn and Te atoms (Ba, Ti, and O atoms for BTO) following the displacement patterns of the soft modes and monitor the total energy variations. Figures 2(a) and 2(b) show the density functional theory (DFT) potential curves along one FE mode of the cubic bulk (as the reference structure) in the bulk and the 1-4UC films of SnTe and BTO, respectively. The bulk results are approached in the two materials upon increasing the film layers, whereas different evolutions are observed. In 1-4UC films of SnTe, the deeper potential wells permit larger instabilities for soft modes, implying an enhancement of T_c in the films. Moreover, the abnormal weakening of this softening feature in the 1UC film compared with the 2-4UC films suggests a nonmonotonic variation of the T_c in 1-4UC films. In BTO, the FE soft mode is monotonically weakened in the films, implying a conventional scaling behavior. The dashed lines in Figs. 2(c) and 2(d) are results obtained using only the first two terms in Eq. (2), shown to highlight the importance of $E_{\mathrm{corr}}^{(d_m)}$ in Eq. (3). Without the correction term $E_{\mathrm{corr}}^{(d_m)}$, the total for SnTe in Eq. (2) is clearly off the trend of

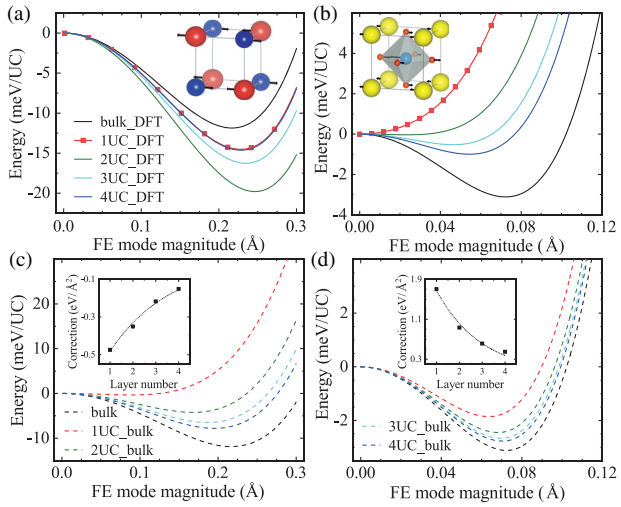

FIG. 2. The potential energy curves of bulk and 1-4UC thin films by DFT for (a) SnTe and (b) BTO. The insets in (a) and (b) indicate the used bulk FE mode. The bottom panels show the same curves using Eq. (2) only with the first two terms for (c) SnTe and (d) BTO. The insets in (c) and (d) show the magnitude of the quadratic corrections in Eq. (3).

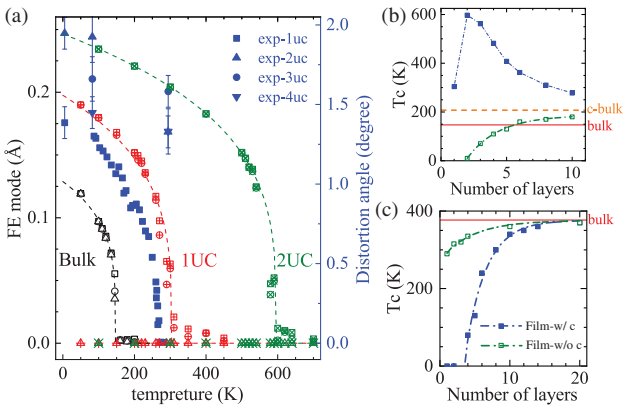

FIG. 3. (a) The phase transitions in bulk, 1UC, and 2UC thin films of SnTe (in black, red, and green open marks, respectively). The order parameters, u_x, u_y, and u_z, are characterized by a square, sphere, and triangle, respectively. In bulk, $u_x = u_y = u_z \neq 0$ in the FE phase. In films, $u_x = u_y \neq 0$ and $u_z = 0$ in the FE phase. Blue solid marks show the experimental data acquired from Ref. [15]. Thickness dependency of T_c is show in (b) for SnTe and in (c) for $BaTiO_3$. Blue (olive) curves show the case with (without) considering $E_{\mathrm{corr}}^{(d_m)}$. The orange horizontal dashed line in (b) is the T_c of the bulk with u_z constrained to zero.

DFT curves [Fig. 2(c)]. For BTO it differs quantitatively [Fig. 2(d)]. $E_{\mathrm{corr}}^{(d_m)}$ represents the intrinsic changes of the electronic structures upon changing from bulk to thin films [20]. Its magnitude as a function of layers is shown in the inset of Figs. 2(c) and 2(d). The different roles played by $E_{\mathrm{corr}}^{(d_m)}$ in SnTe and BTO are crucial for their scaling behaviors. These static DFT results are in alignment with the experiments in Ref. [15]. However, considering the complicated 2D nature, e.g., fluctuations are enhanced by truncated geometry, they are not sufficient to clarify the full picture of the FE phase transitions in thin films at finite T's. Thermodynamical stability among phases should be concerned. This is done by using the aforementioned effective Hamiltonian in performing finite-T Monte Carlo simulations.

We first look at the bulk PE-FE phase transitions in SnTe and BTO. SnTe turns from cubic PE phase (Fm-3m) to rhombohedral ($R3m$) FE phase at 98 K [21]. Our simulations reproduce this by giving a T_c of 147 K, which is identified by the temperature dependency of FE modes [black marks in Fig. 3(a)]. A difference of ~50 K is left to account for the defects effect, which is absent in our perfect crystal simulations [23,24]. Our simulations also obtain reasonable $T_c \sim 370$ K for bulk BTO transiting from cubic PE phase (Pm-3m) to tetragonal FE phase ($P4mm$) (Fig. S4), consistent with published studies [49,50].

Then we check T_c at varying layers. Deviated from bulk, the SnTe monolayer prefers in-plane polarization (along [110] direction) [51], as shown by red marks in Fig. 3(a). We observed a transition from the PE tetragonal phase to the FE monoclinic phase. This in-plane polarization in monolayer is robust even at room T, appealing for practical ultrathin devices. Besides this, the thickness dependency of T_c is also in alignment with the experimental observations, which measure the distortion angles [Fig. 3(a) scale to right in blue]. This can be seen by comparing the trend of saturated distortion angle with FE modes from our simulations. They are smaller in 1UC than in 2UC [from red to green symbols scaling to left in Fig. 3(a)]. After 2UC, they decrease and approach the bulk value from above. More alignments can be found in the magnitude of saturated distortion angle ~1.2° (exp. ~1.4°), and the critical index 0.27–0.35 for 1-4UC films (exp. 0.33 ± 0.05); see Supplemental Material [35]. T_c shows the same nonmonotonic trend in clear discrepancy with the conventional scaling law [blue curves in Fig. 3(b)], whereas it holds in BTO [Fig. 3(c)].

Last but not least, threats from extrinsic effects should be ruled out or controlled. Experiments on SnTe bulk show that T_c drops with increasing carrier concentration [23,24]. Enhancement in T_c as several tens of Kelvin would be expected from the fabricated high quality samples to the defect-free materials. Considering the fact we reproduce the abnormal scaling behavior of SnTe upon using stoichiometric structure, the effects of free carriers (Sn vacancies) should be minor. Strain effects, however, are crucial and might dramatically tune T_c shown by early studies in perovskites [16,52,53]. Since our model exhibits a built-in stress-strain relation, we set the same external pressure and fully relax the films in the MC simulations. For more discussions on these extrinsic effects, please see Supplemental Material [35]. In so doing, we claim the abnormalities in SnTe are an intrinsic size effect with an underlying mechanism to be revealed.

To understand this abnormality, we compare the microscopic details of the PE-FE phase transitions in SnTe and in BTO. In bulk BTO, four phases from cubic (C) through tetragonal (T) and orthogonal (O) to rhombohedral (R) exist upon decreasing T's, and polarizations along x, y, and z appear sequentially [Fig. 4(a)]. In BTO thin films, depolarization results in zero polarization along z. Three phases from quasicubic (QC) through quasitetragonal (QT) to quasiorthogonal (QO) exist at decreasing T's, and polarizations along x and y appear sequentially. In both cases, T_c corresponds to the same physical process (symmetry breaking here) that only one of the three FE modes is softened [Fig. 4(a)], i.e., C-T phase transition in bulk and the QC-QT one in thin films. From bulk to thin films, the finite film thickness cuts off long-distance correlations along z of the in-plane polarizations so that an appreciable finite-size rounding of critical-point singularities is to be expected [11]. This forms the aforementioned basis of FSS theory [7], and conventional scaling behavior is expected.

This situation, however, is different in SnTe where T_c corresponds to different physical processes, as discussed. The PE-FE transition is C-R in bulk and QC-QO in films. The QC-QO transition in films corresponds to the C-O transition in bulk, which does not appear spontaneously. Utilizing the knowledge of BTO's phase sequence, if C-O exists, it should occur at a higher T. By convenience of our simulations, we can verify this by constraining the FE mode along z direction $u_z = 0$. This allows us to artificially obtain the C-O transition sequence in bulk, as shown in Fig. 4(b). When the PE-FE transition is forced to happen between C and O phases, the T_c is substantially elevated. Therefore, the elevated T_c in the films is related to this omitted O phase in bulk. The FSS theory aims to describe the scaling behavior between universality classes only deviated in spatial dimensionality, which presumes the same physical process, characterized by the same order parameters and formulation of interactions upon scaling the system size. This prerequisite is not fulfilled in SnTe. The order parameters clearly change since the triply degenerate FE modes cannot soften simultaneously in the films.

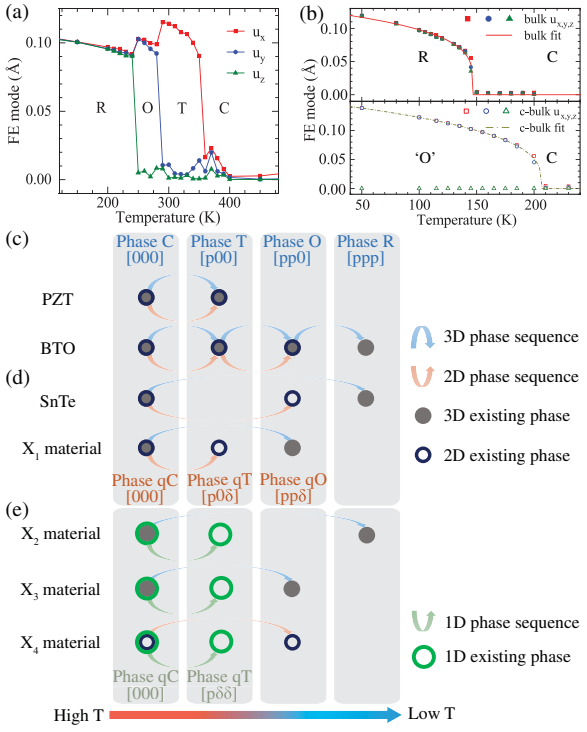

FIG. 4. (a) The C-T-O-R transition sequence in bulk BTO. (b) Top panel: the spontaneous C-R phase transition in bulk SnTe. Bottom panel: the artificial C-O phase transition in bulk SnTe by constraining $u_z = 0$. Schematic of the transition sequence for (c) the conventional FE materials including BTO and PZT, (d) 2D anomaly including SnTe, and (e) 1D anomaly based on the same mechanism remaining to be explored. X_1 to X_4 label candidates for robust low-dimensional FE devices.

These different scaling behaviors can also be understood by looking at the role played by $E_{\mathrm{corr}}^{(d_m)}$ in Eq. (2). In BTO, the quantitative changes in electronic structure do not result in a qualitative change of their relative positions upon going from the films to bulk, while this is not the case in SnTe [Figs. 2(a) and 2(c)]. In Refs. [7,54,55], when the scaling law is deduced, a model Hamiltonian (e.g., the Ising model) is chosen and the difference between the bulk and films is characterized by geometric changes. Renormalization group theory is used and the subtle but crucial changes of the Hamiltonian upon going from bulk to films are neglected. This assumption is violated seriously in SnTe. To test this, we can choose the first two terms in Eq. (2), which addressed the geometric changes but not the electronic structures, to perform the PE-FE phase transition upon going from bulk to films. The scaling law becomes valid again in both SnTe and BTO [olive curves in Figs. 3(b) and 3(c)]. Therefore, when the changes of electronic structures result in a qualitative change of the Hamiltonian itself, the scaling law fails. One macroscopic observable to characterize this abnormality is the order parameters related to symmetry as we have discussed.

Using this picture, we now propose some promising low-dimensional FE materials with higher T_c than their higher-dimensional correspondences. The jumping transition sequence in Figs. 4(d) and 4(e) could help. Intuitively, this means highly degenerate FE modes, which can soften simultaneously in the higher-dimensional systems. With decreasing dimensionality, symmetry breaking eliminates this simultaneous softening. Thereby, one can expect different order parameters for bulk and films, and higher T_c beyond the scaling law limit. In bulk, a C-T-O-R sequence of phase transition might happen upon decreasing T's. This corresponds to a QC-QT-QO sequence in films, and a QC-QT sequence in 1D systems. Upon going from 3D to 2D, Fig. 4(c) shows the case when nothing was jumped in bulk, including BTO and $Pb[Zr_xTi_{1-x}]O_3$ (PZT). In SnTe, the T and O phases were jumped. Besides this,

when the 3D PE-FE phase transition happens between C and O, the T phase can be jumped [X_1 in Fig. 4(d)]. This picture might also apply to the 3D to 1D and 2D to 1D transitions. Three possibilities are shown in Fig. 4(e). When the 3D PE-FE transition happens between C and R (or C and O), the T and O phases (T phase) are jumped in bulk, labeled by X_2 (X_3). When the 2D PE-FE transition happens between QC and QR, the QT phase is jumped in the films [X_4 in Fig. 4(e)]. These suggestions based on symmetry provide a simple rule of thumb to seek systems in which the low-dimensional systems can possess higher T_c than their higher-dimensional correspondences. Accurate numerical characterizations, however, need to resort to the first-principles based finite-T simulations as reported above. Considering the fundamental importance of FE size effect and phase transition problems in condensed matter physics, we hope this work can stimulate more experimental and theoretical studies in this direction.

The authors are supported by the National Basic Research Programs of China under Grant No. 2016YFA0300900, and the National Science Foundation of China under Grants No. 11774003, No. 11604092, and No. 11634001, and No. 51672007. We sincerely thank Professor Zhirong Liu and Professor Wenhui Duan for insightful discussions. The computational resources were supported by the high-performance computing platform of Peking University, China.

*xzli@pku.edu.cn

[1] J. Junquera and P. Ghosez, Nature (London) **422**, 506 (2003).
[2] N. A. Spaldin, Science **304**, 1606 (2004).
[3] C. H. Ahn, K. M. Rabe, and J.-M. Triscone, Science **303**, 488 (2004).
[4] M. Dawber, K. M. Rabe, and J. F. Scott, Rev. Mod. Phys. **77**, 1083 (2005).
[5] J. F. Scott, Science **315**, 954 (2007).
[6] L. W. Martin and A. M. Rappe, Nat. Rev. Mater. **2**, 16087 (2016).
[7] M. E. Fisher and M. N. Barber, Phys. Rev. Lett. **28**, 1516 (1972).
[8] K. Binder and P. C. Hohenberg, Phys. Rev. B **9**, 2194 (1974).
[9] F. Huang, G. J. Mankey, M. T. Kief, and R. F. Willis, J. Appl. Phys. **73**, 6760 (1993).
[10] The scaling law is sometimes written in a similar form suggested to better fit the experimental data, as $\delta T_c'(d) = [T_c(\infty) - T_c(d)]/T_c(d) = (\xi_0'/d)^{\lambda'}$.
[11] V. Privman, in *Finite Size Scaling and Numerical Simulation of Statistical Systems* (World Scientific, Singapore, 1990), pp. 1–98.
[12] D. D. Fong, G. B. Stephenson, S. K. Streiffer *et al.*, Science **304**, 1650 (2004).
[13] I. A. Kornev, H. Fu, and L. Bellaiche, J. Mater. Sci. **41**, 137 (2006).
[14] E. Almahmoud, I. Kornev, and L. Bellaiche, Phys. Rev. B **81**, 064105 (2010).
[15] K. Chang, J. Liu, H. Lin *et al.*, Science **353**, 274 (2016).
[16] R. Fei, W. Kang, and L. Yang, Phys. Rev. Lett. **117**, 097601 (2016).
[17] M. Wu and X. C. Zeng, Nano Lett. **16**, 3236 (2016).
[18] M. Mehboudi, B. M. Fregoso, Y. Yang, W. Zhu, A. vanderZande, J. Ferrer, L. Bellaiche, P. Kumar, and S. Barraza-Lopez, Phys. Rev. Lett. **117**, 246802 (2016).
[19] W. Wan, C. Liu, W. Xiao, and Y. Yao, Appl. Phys. Lett. **111**, 132904 (2017).
[20] K. Liu, J. Lu, S. Picozzi, L. Bellaiche, and H. Xiang, Phys. Rev. Lett. **121**, 027601 (2018).
[21] M. Iizumi, Y. Hamaguchi, K. F. Komatsubara, and Y. Kato, J. Phys. Soc. Jpn. **38**, 443 (1975).
[22] P. Z. Hanakata, A. Carvalho, D. K. Campbell, and H. S. Park, Phys. Rev. B **94**, 035304 (2016).
[23] S. Sugai, K. Murase, S. Katayama, S. Takaoka, S. Nishi, and H. Kawamura, Solid State Commun. **24**, 407 (1977).
[24] K. L. I. Kobayashi, Y. Kato, Y. Katayama, and K. F. Komatsubara, Phys. Rev. Lett. **37**, 772 (1976).
[25] F. W. de Wette, W. Kress, and U. Schröder, Phys. Rev. B **32**, 4143 (1985).
[26] G. A. Samara, T. Sakudo, and K. Yoshimitsu, Phys. Rev. Lett. **35**, 1767 (1975).
[27] W. Zhong, D. Vanderbilt, and K. M. Rabe, Phys. Rev. B **52**, 6301 (1995).
[28] L. Bellaiche and D. Vanderbilt, Phys. Rev. B **61**, 7877 (2000).
[29] L. Bellaiche, A. Garcia, and D. Vanderbilt, Phys. Rev. Lett. **84**, 5427 (2000).
[30] I. Kornev, H. Fu, and L. Bellaiche, Phys. Rev. Lett. **93**, 196104 (2004).
[31] B. Meyer and D. Vanderbilt, Phys. Rev. B **65**, 104111 (2002).
[32] T. Nishimatsu, U. V. Waghmare, Y. Kawazoe, and D. Vanderbilt, Phys. Rev. B **78**, 104104 (2008).
[33] I. A. Kornev, L. Bellaiche, P. Bouvier, P. E. Janolin, B. Dkhil, and J. Kreisel, Phys. Rev. Lett. **95**, 196804 (2005).
[34] L. Chen, Y. Yang, Z. Gui, D. Sando, M. Bibes, X. K. Meng, and L. Bellaiche, Phys. Rev. Lett. **115**, 267602 (2015).
[35] See Supplemental Material at http://link.aps.org/supplemental/10.1103/PhysRevLett.121.135702 for details of the method and computational setups, which includes Refs. [36–43].
[36] M. P. Allen and D. J. Tildesley, *Computer Simulation of Liquids* (Oxford University Press, Clarendon, 2017), Vol. 1, p. 267.
[37] G. Kresse and J. Furthmüller, Phys. Rev. B **54**, 11169 (1996).
[38] G. Kresse and D. Joubert, Phys. Rev. B **59**, 1758 (1999).
[39] A. Togo and I. Tanaka, Scr. Mater. **108**, 1 (2015).
[40] D. M. Ceperley and B. J. Alder, Phys. Rev. Lett. **45**, 566 (1980).
[41] J. P. Perdew, K. Burke, and M. Ernzerhof, Phys. Rev. Lett. **77**, 3865 (1996).
[42] J. Sun, A. Ruzsinszky, and J. P. Perdew, Phys. Rev. Lett. **115**, 036402 (2015).
[43] K. M. Rabe and J. D. Joannopoulos, Phys. Rev. Lett. **59**, 570 (1987).

[44] A. Grzybowski and A. Bródka, Chem. Phys. Lett. **361**, 329 (2002).
[45] E. Almahmoud, Y. Navtsenya, I. Kornev, H. Fu, and L. Bellaiche, Phys. Rev. B **70**, 220102 (2004).
[46] R. D. King-Smith and D. Vanderbilt, Phys. Rev. B **47**, 1651 (1993).
[47] R. Resta, M. Posternak, and A. Baldereschi, Phys. Rev. Lett. **70**, 1010 (1993).
[48] Here we talk about the Curie temperature related FE phase of BTO, namely, the tetragonal phase. There are two other FE phases, where [110] and [111] polarizations require more FE modes involved.
[49] W. Zhong, D. Vanderbilt, and K. M. Rabe, Phys. Rev. Lett. **73**, 1861 (1994).
[50] L. Walizer, S. Lisenkov, and L. Bellaiche, Phys. Rev. B **73**, 144105 (2006).
[51] N. Huang, Z. Liu, Z. Wu, J. Wu, W. Duan, B. L. Gu, and X. W. Zhang, Phys. Rev. Lett. **91**, 067602 (2003).
[52] J. H. Haeni, P. Irvin, W. Chang *et al.*, Nature (London) **430**, 758 (2004).
[53] K. J. Choi, M. Biegalski, L. Y. Li *et al.*, Science **306**, 1005 (2004).
[54] M. E. Fisher, Rev. Mod. Phys. **46**, 597 (1974).
[55] K. G. Wilson, Rev. Mod. Phys. **55**, 583 (1983).